# Entropy Generation in Hydromagnetic Thermal Boundary Layer Flow of Micropolar Fluid Over a Convectively Heated Nonlinear Stretching Sheet

**E. O. Fatunmbi[1], S. O. Bello[2]**

[1-2]Department of Mathematics and Statistics, Federal Polytechnic, Ilaro, Nigeria.
E-mail: [1]ephesus.fatunmbi@federalpolyilaro.edu.ng, [2]sikiru.bello@federalpolyilaro.edu.ng
Corresponding e-mail: *ephesus.fatunmbi@federalpolyilaro.edu.ng

**Abstract**

The optimal use of energy is the critical objective in the building of thermal devices which are useful both in engineering and industrial operations. To achieve this objective, considerable attention should be paid to minimization of entropy production in the processes. In view of this, entropy generation in thermal boundary layer fluid flow of an electrically conducting micropolar fluid over a convectively heated nonlinear stretching sheet being influenced by viscous dissipation and thermal radiation has been analyzed in this study. The formulated governing equations of the flow, heat transfer and entropy generation are converted to ordinary differential equations by similarity transformation procedures. Thereafter, the resulting equations are computationally integrated by means of shooting techniques accompanied by fourth order Runge-Kutta algorithms entrenched in a symbolic software Maple 2016. The imapct of various controlling physical parameters on the fluid flow, temperature distribution, entropy generation, Bejan number and other quatities of engineering interest are discussed through graphs and tables. The facts from the study show that heat transfer irreversibility is stronger than that of viscous dissipation and Joule heating as the radiation parameter rises while the nonlinear stretching parameter influence is to diminish the transfer of heat..

**Keywords**: Bounadary layer; convective heating; entropy production; micropolar fluid; nonlinear stretching sheet

## 1.0 Introduction

The power and benefits of non-Newtonian fluids in industrial and engineering processes have motivated quite a number of researchers and scientists in the recent times to pay more attention to its study. Different from Newtonian fluids, the viscosity of non-Newtonian fluids is dependent on the shear rate or shear rate history. Examples of such fluids are ketchup, butter, cosmetics, polymer solutions, blood, colloids, mud flows and gels. The applications of such fluids are germane in nature and manufacturing operations which include; crude oil extraction, food and polymer processing, chemical processing, blood flow, polymer extrusion, bio-mechanic engineering, etc (Panigrahi, Reza and Mishra, 2015; Anuradha and Punithavalli, 2019).

However, owing to diverse fluid propertities in nature, there exists no single constitutive model that can capture effectively the non-Newtonian fluids characteristics. In view of this, different non-Newtonian fluid concept have been developed based on different physical characteristics. Such models include the micropolar fluid, Maxwell fluid, Johnson-Segalman fluid, Casson fluid, Jeffery fluid, etc (Chen, Liang, and Lee, 2011). The micropolar fluid has become popular and interesting area of research among other non-Newtonian fluids due to its ability to describe effectively fluids with microstructure. Erigen (1966, 1972) formulated the theory of micropolar fluid and thermal-micropolar fluid respectively.

The micropolar fluid describes fluids which manifest some microscopic influence emanating from the local structure and micromotion of its particles. Physically, they consist of rigid, spherical or

bar-like particles suspended in a viscous medium (Lukaszewicz, 1999). Such fluids include the polymeric and fluid suspensions, animal blood, liquid crystals, colloidal fluids, etc (Hayat, Mustafa and Obaidat, 2011). They offered mathematical framework for analyzing various complex and complicated fluids including polymeric, colloidal fluids and suspension solutions which cannot be described effectively by the Navier-Sotkes model. Besides, there are huge scientific and industrial usage of such fluids such as in extrusion of polymer fluids, the cooling of metallic plate in water bath, synovial lubrication, arterial blood flows, sediment transport in rivers (Rahman, 2009; Reena and Rana, 2009).

The investigation of boundary layer flow passing stretching sheet provide significant applications in manufacturing and engineering works such as in textile and paper production, extrusion of plastic sheet and metal, drawi ng of copper wires, glass blowing, drawing of plastic films. This kind of study was initiated by Sakiadis (1961) and has since been explored by various scholars (see Crane, 1970; Fatunmbi and Adeniyan, 2018; Makinde, *et al.*, 2018). Practically, the sheet could be stretched nonlinearly as reported by Gupta and Gupta (1977). This kind of study has been addressed by Vajravelu (2001); Cortell (2008); Hayat (2008); Panigrahi, Reza and Mishra, (2015), Waqas *et al.*, (2016) with various parameters of interest, different methods and wall conditions. In all these studies however, only Newtonian fluids are applied while non-Newtonian fluids especially the micropolar fluid have been ignored inspite of its usefulness.

Meanwhile, the boundary layer flow and heat transfer charateristics over a stretching sheet with the use of micropolar fluids have been reported by various researchers (see Chaudhary and Jha, 2008; Fatunmbi and Fenuga, 2017; Kamran, 2018; Arifuzzaman *et al*., 2018) while checking the impact of various parameters, geometries under different condtions and assumptions. Howbeit, these studies have only been devoted to thermodynamics first law only. Kobo and Makinde (2010) however reported that studies conducted with thermodynamics second law corresponding to entropy generation are dependable than those the first law. Entropy generation is a means of determining the irreversibility that occur in a themodynamical system in order to upgrade such system ( Makinde, 2012).

The study of entropy generation has become consequential because in many engineering as well as industrial works, the generation of entropy leads to the destruction of available energy in the sysytem. The performance of thermal machines such as air conditioners, power plants, heat pumps, refrigerator, etc can be determined by the rate of entropy generation. Hence, it becomes necessary to investigate such phenomenon through the use of second law of thermodynamics with a view to optimize the energy in the system for effective performance. On the ground of crucial relevance of such studies in engineering and industrial works, quite a number of reseachers (see Bejan, 1982, 1996; Rashidi and Abbas, 2017; Ishaq *et al*., 2018; Salawu *et al.*, 2019; Salawu and Fatunmbi, 2017; Srinivasacharya and Bindu, 2017; Makinde and Eegunjobi, 2018; El-Aziz, and Saleem, 2019) have addressed such problem on both Newtonian and non-Newtonian fluids. None of these studies however has been conducted with the use of micropolar fluid over a convectively heated nonlinear stretching sheet.

Hence, the focus of this study is to address numerically entropy generation in hydromagnetic thermal boundary layer fluid flow of micropolar type along a nonlinear stretching sheet with convective wall condition. The impact of thermal radiation, varying heat source and viscous dissipation are also checked owing to their usefulness in engineering and industrial processes including gas turbines, astrophysical flows, power plants, etc

## 2.0 Mathematical Development of the Model

For the formulation of the model and to develop the governing equations, it is assumed that the flow is steady, two-dimensional, incompressible, viscous with Cartesian coordinate $(x, y, z)$ having corresponding velocity components $(u, v, 0)$. The flow is also assumed to be in $x$ direction while $y$ axis is normal to it. The working fluid is taken to be electrically conducting, radiating and dissipative non-Newtonian micropolar fluid which flow over a convectively heated impermeable nonlinear stretching sheet with velocity $u = U_0 x^p$ where $U_0$ is a positive constant and $p$ is the power law stretching parameter. A transverse magnetic field of strength $B_0$ is applied normal to the flow direction as depicted in Fig. 1 while the induced magnetic field and electric field have been neglected. The fluid flow properties are assumed to be isotropic and constant and the sheet temperature is upheld by a convective heating process from a hot fluid of a temperature $T_f$. The impact of Joule heating as well as viscous dissipation and thermal radiation are also checked on the model.

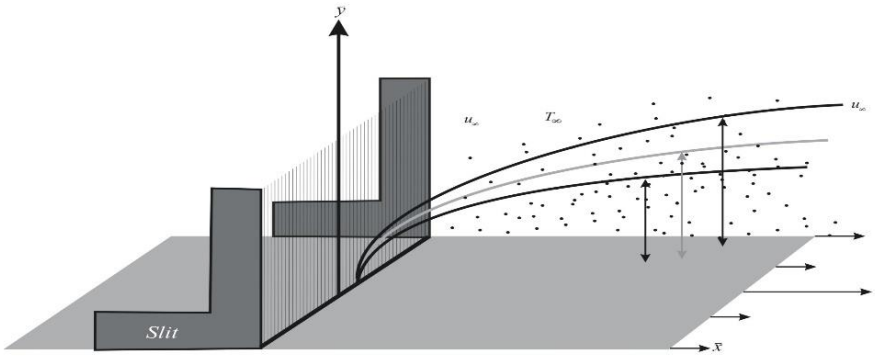


**Fig. 1**.The Sketch of the Physical Model

In view of the assumptions stated above and with the use of boundary layer approximations, the governing equations are

$$\frac{\partial u}{\partial x} + \frac{\partial v}{\partial y} = 0, \tag{1}$$

$$u\frac{\partial u}{\partial x} + v\frac{\partial u}{\partial y} = \frac{1}{\rho}(\mu + r)\frac{\partial^2 u}{\partial y^2} + \frac{\mathrm{r}}{\rho}\frac{\partial H}{\partial y} - \frac{\sigma \mathrm{B}_0^2}{\rho}u \tag{2}$$

$$u\frac{\partial H}{\partial x} + v\frac{\partial H}{\partial y} = \frac{\gamma}{\rho j}\frac{\partial^2 H}{\partial y^2} - \frac{r}{\rho j}\left(2H + \frac{\partial u}{\partial y}\right), \tag{3}$$

$$u\frac{\partial T}{\partial x} + v\frac{\partial T}{\partial y} = \frac{k}{\rho c_p}\left(1 + \frac{16\sigma^* T_\infty^3}{3k^* k}\right)\frac{\partial T^2}{\partial y^2} + \frac{(\mu + r)}{\rho c_p}\left(\frac{\partial u}{\partial y}\right)^2 + \frac{\sigma \mathrm{B}_0^2}{\rho c_p}u^2 + \frac{p'''}{\rho c_p}, \tag{4}$$

The non-uniform heat source/sink $p'''$ in Eq. (4) is expressed as

$$p''' = \frac{k u_w}{x^p \nu}\left(T_f - T_\infty\right)[A_1 f' + \mathrm{A}_2\theta], \tag{5}$$

Where $A_1 = \alpha x^{p-1}$ and $A_2 = \beta^{\star} x^{p-1}$ are space and heat dependent source/sink respectively such that $A_1 > 0,\ A_2 > 0$ relates to heat source while $A_1 < 0, A_2 < 0$ implies heat sink.
The relevant boundary conditions for the governing equations are:

$$\begin{aligned} &u = u_w = U_0 x^p, v = 0,\ H = 0, -\frac{k\partial T}{\partial y} = \mathrm{h_f}\left(T_f + T_\infty\right) at\ y = 0, \\ &u \to 0, H \to 0, T \to T_\infty\ as\ y \to \infty. \end{aligned} \tag{6}$$

The various symbols used in the governing equatuons are summarised in Table 1 with their nonmenclature.

**Table 1**: Symbols and their nonmenclature

| Symbols | Nomenclature | Symbols | Nomenclature |
|---|---|---|---|
| $u$ | Velocity in $x$ direction | $T$ | Temperature |
| $v$ | Velocity in $y$ direction | $h_f$ | Coefficient of heat transfer |
| $\rho$ | Fluid density | $T_f$ | Surface sheet temperature |
| $\mu$ | Newtonian viscosity | $u_w$ | Velocity at the sheet |
| $r$ | Vortex viscosity | $U_0$ | Nonlinear stretching velocity |
| $\sigma_0$ | Electrical conductivity | $j$ | Micro inertial density |
| $c_p$ | Specific heat capacity | $\gamma$ | Spin gradent viscosity |
| $k$ | Thermal conductivity | $T_\infty$ | Temperature at free stream |
| $\sigma^{\star}$ | Stefan-Boltzmann constant | $k^{\star}$ | Mean absorption coefficient |
| $p'''$ | Non-uniform heat source | $H$ | Microrotation component |

### 2.1 The Model Transformation

To simplify further the governing equations, we applied similarity transformation variables (see Salem, 2013) in Eq. (7) such that the continuity Eq. (1) is satisfied with the use of the stream function $u$ and $v$ defined in (7)

$$\begin{aligned} &\eta = y\left[\frac{U_0(p+1)x^p}{2x\nu}\right]^{1/2}, H = x^{(3p-1)/2}\left[\frac{U_0^3(p+1)}{2\nu}\right]^{1/2} g(\eta), \\ &u = \frac{\partial\psi}{\partial y} = U_0 x^p f', v = -\frac{\partial\psi}{\partial x} = -\left[\frac{U_0\nu(p+1)}{2}\right]^{\frac{1}{2}} x^{\frac{p-1}{2}}\left(f + \frac{(p-1)}{(p+1)}\eta f'\right), \\ &\gamma = \left(\mu + \frac{r}{2}\right) j, \theta(\eta) = \frac{T-T_\infty}{T_w - T_\infty}, j = \left(\frac{\nu}{U_0}\right) x^{(1-p)}. \end{aligned} \tag{7}$$

With the substitution of Eq. (7) into Eqs. (2-4) aand taking cognizance of Eq. (5), the Eqs. describing the flow, microrotation and energy in ordinary differential forms are listed below

$$(1+K)f''' + ff'' + Kg' - \left(\frac{2}{p+1}\right)[(p+M)f'^2] = 0, \tag{8}$$

$$(1 + K/2)g'' + fg' - \left(\frac{3p-1}{p+1}\right)f'g - (2g + f'')\left(\frac{2K}{p+1}\right) = 0, \tag{9}$$

$$\begin{aligned} &(1+R)\theta'' - \left(\frac{2}{p+1}\right)Prf'\theta + Prf\theta' + (1+K)PrEcf''^2 + \\ &\left(\frac{2}{p+1}\right)PrMEcf'^3 + \left(\frac{2}{p+1}\right)(\alpha f' + \beta\theta) = 0. \end{aligned} \tag{10}$$

Tthe boundary conditions (6) also translate to

$$f'(0)=1, f(0)=0, g(0)=0, \theta'(0)=\zeta(\theta(0)-1),$$
$$f'(\infty)=0, g(\infty)=0, \theta(\infty)=0. \tag{11}$$

Where

$$\zeta=\frac{h_f}{k}\left[\frac{2\nu}{U_0(p+1)}\right]^{0.5},\ M=\frac{\sigma_0 B_0^2}{\rho}, \alpha=\frac{bk}{\mu c_p}, \beta=\frac{b^\star k}{\mu c_p}$$
$$R=\frac{16T_\infty^3\sigma^\star}{3k^\star k}, K=\frac{r}{\mu}, Ec=\frac{u_w^2}{cp(T_w-T_\infty)}, Pr=\frac{\mu c_p}{k}. \tag{12}$$

For the engineering community, the relevant quantities of concern are the skin friction coefficient and the Nusselt number which are written respectively in Eq. (13)

$$C_{fx}=\frac{\tau_w}{\rho u_w^2}, Nu_x=\frac{xq_w}{k(T_w-T_\infty)}, \tag{13}$$

where $\tau_w$ and $q_w$ are respectively described in Eq. (14) as

$$\tau_w=\left[(\mu+r)\frac{\partial u}{\partial y}+rH\right]_{y=0}, q_w=-\left[\left(k+\frac{16T_\infty^3\sigma^\star}{3k^\star}\right)\frac{\partial T}{\partial y}\right]_{y=0}. \tag{14}$$

Upon substituting Eqs. (7) and (14) in (13), the skin friction coefficient becomes

$$C_{fx}=\left(\frac{p+1}{2}\right)^{\frac{1}{2}}(1+K)Re_x^{-1/2}f''(0), \tag{15}$$

while the Nusselt number translates to

$$Nu_x=-(1+R)\left(\frac{p+1}{2}\right)^{1/2}Re_x^{1/2}\theta'(0) \tag{16}$$

The differentiation in the governing Eqs. is carried out with respect to $\eta$ where $\eta$ is the similarity transformation variable. The description of various parameters incoporated in Eqs. (10-18) are summarised in Table 2.

**Table 2**: The description of the parameters used

| Parameter | Description |
|---|---|
| $K$ | Material parameter |
| $p$ | Nonlinear stretching parameter |
| $M$ | Magnetic field parameter |
| $R$ | Radiation parameter |
| $Pr$ | Prandtl number |
| $Ec$ | Eckert number |
| $\alpha$ | Space-dependent heat source |
| $\beta$ | Temperature-dependentheat source |
| $\zeta$ | Biot number (convective heating parameter) |
| $t_w$ | Surface shear stress |
| $q_w$ | Surface heat flux |
| $C_{fx}$ | Skin friction coefficient |
| $Nu_x$ | Nusselt number |

## 3.0 Entropy Generation

The volumetric rate of entropy production in hydromagnetic thermal boundary layer micropolar fluid flow with dissipative and radiative properties are described as follows (see Afridi, 2017).

$$S_{gen} = \frac{k}{T^2}\left[(\nabla T)^2 + \frac{16\sigma^{\star}T_{\infty}^3}{3k^{\star}k}(\nabla T)^2\right] + \frac{(\mu+r)}{T}\left(\frac{\partial u}{\partial y}\right)^2 + \frac{\sigma B_0^2}{T}u^2. \tag{17}$$

In line with Bejan (1979), the non-dimensional entropy production number is the described by the ratio of the volumetric production of entropy and the characteristic rate of entropy generation. Thus, by means of the similarity quantities (7) and on the assumptionn of linear surface, then Eq. (17) becomes

$$E_g = \frac{S_{gen}}{S_{gc}} = \frac{(1+R)\theta\prime^2}{(\theta+\Omega)^2} + \frac{PrEc}{(\theta+\Omega)}(1+K)f''^2 + \frac{2PrEcM}{(\theta+\Omega)}f'^3, \tag{18}$$

Here the overall entropy production in the system is denoted by $E_g$ while $S_g = kU_0/\nu$ stands for the characteristic entropy production and $\Omega = T_{\infty}/(T_w - T_{\infty})$ describes the non-dimensional temperature difference. The Bejan number is used to describe the proportion of the entropy production by heat transfer to the total proportion in a system as represented in Eq. (19). The first term in Eq. (17 or 18) indicates production of entropy resulting from heat transfer ($N_H$), the second term describes entropy due to viscous dissipation ($N_V$) because of fluid friction and the third term represents generation of entropy by Joule heating ($N_J$).

$$Be = \frac{N_H}{Eg} = \frac{N_H}{N_H+N_V+N_J}, \tag{19}$$

where $N_H, N_V$ and $N_J$ depict entropy production due to heat transfer, viscous dissipation and Joule heating in that order whereas $Be$ is stands for the Bejan number which varies in the interval $0 \leq Be \leq 1$. The dominance of the parameters $N_V + N_J$ over $N_H$ happens when $Be = 0$, the implication of this is that entropy production as a result of heat transfer ($N_H$) is dominated by those of viscous dissipation and Joule (Ohmic heating) ($N_V + N_J$). Meanwhile, the value of $Be = 1$ implies that generation of entropy owing to heat transfer is dominant over that of viscous dissipation and Joule heating whereas the value of $Be = 1/2$ points to the fact that $N_H = N_V + N_J$.

## 4.0 Solution Method and Result Validation

The ordinary differential Eqs. (8-10) together with the boundary conditions (11) form a boundary value problem which are coupled and highly nonlinear in nature. In this regard, numerical solutions have been employed to profer results to the governing Eqs. (8-10). To achieve this, shooting techniques together with fourth order Runge-Kutta scheme on a computer algebra symbolic Maple 2016 package have been engaged. The validity of the numerical codes have been tested by verifying the computional results obtained with the related existing results in literature to ascertain the level of accuracy of the solution in the limiting cases. The values of the skin friction coefficient $C_{fx}$ are compared with those reported by Ulla *et al.* (2017) and Lu *et al.* (2018) for different values of the nonlinear stretching parameter $p$. The comparisons demonstrate good relationship as displayed in Table 3. From this table also, it is observed that higher values of the nonlinear stretching parameter $p$ encourage the growth of the skin friction coefficient $C_{fx}$.

**Table 3:** Computed values of $C_{fx}$ as compared with existing results for variation in $p$ when $K = Ec = M = \alpha = \beta = 0$

| $p$ | Ulla *et al.* (2017) | Lu *et al.* (2018) | Present |
|---|---|---|---|
| 0.0 | 0.6276 | 0.627547 | 0.627563 |
| 0.2 | 0.7668 | 0.766758 | 0.766846 |
| 0.5 | 0.8896 | 0.889477 | 0.889552 |
| 1.0 | 1.0000 | 1.000000 | 1.000008 |
| 1.5 | - | 1.061587 | 1.061609 |
| 3.0 | 1.1486 | 1.148588 | 1.148601 |
| 10.0 | 1.2349 | - | 1.234882 |
| 100.0 | 1.2768 | - | 1.276781 |

## 4.0 Results Analysis and Discussion

For effective analysis and discussion of results we have included graphically the effects of the main controlling parameters on the dimensionless velocity, temperature, entropy generation and Bejan number. The computational values adopted have been carefully selected from the previous related researches such that they are suitable for the present work. In this regard, the parameter values: are $K = 0.5, M = 0.5, Ec = 0.01, p = 0.2 = R, Pr = 0.71, \zeta = 0.2, \alpha = \beta = 0.01$ and $\Omega = 0.5$, unless stated otherwise on the plots.

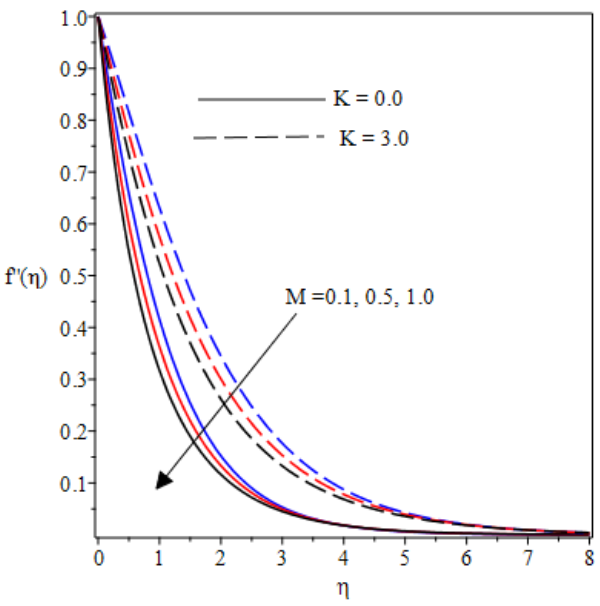


**Fig. 2** Reaction of velocity to changes in $M$ & $K$

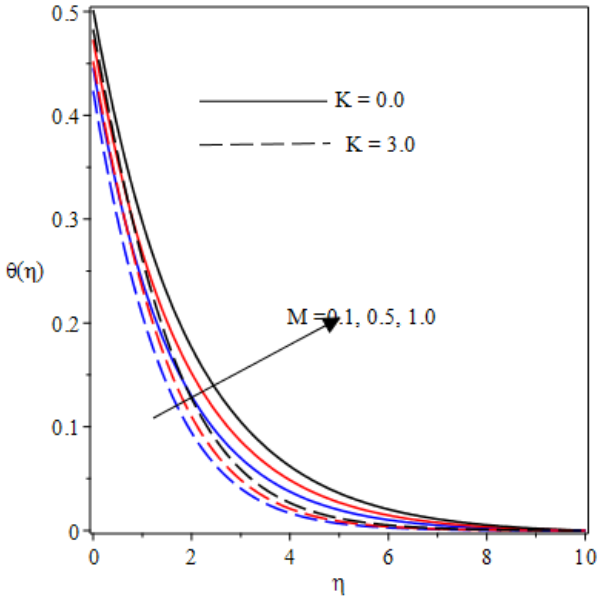


**Fig. 3** Temperature field for varying $M$ & $K$

The plot in Fig. 2 depicts the impact of the magnetic field parameter $M$ on the velocity profile with variation in the micropolar term $K$. It is evident that the velocity field declines with an increase in $M$ both in the presence and and absence of $K$. This response is attributed to the imposition of the

transverse magnetic field on an electrically conducting fluid which create a resistive kind of force known as Lorentz force. This force acts against fluid motion and slowng it down. On the contrary, the introduction of the micropolar fluid enhances the fluid flow, this reaction is due to the lowerinng of the dynamic viscosity as $K$ rises. In Fig. 3 however, the surface temperature appreciates with rising values of the magnetic field parameter. This is due to drag created by the Lorentz force on the flow. The effect of $K$ is to decrease the temperature profile as noted in this figure.

Fig. 4 is the plot of the temperature against $\eta$ for various values of Eckert number Ec for changes in the Prandtl number $Pr$. As the fluid flow occurs, the internal friction due to fluid particles described by viscous dissipation as represented by Ec causes generation of heat and thereby leading to a rise in temperature. On the other hand, the Prandtl number $Pr$ is seen to diminish the thermal boundary layer thickness and consequently causing a decline in the surface temperature. Physically, Prandtl number defines the ratio of momentum diffusivity to that of thermal diffusivity, thus a rise in $Pr$ shows that the convection effect is dominant over conduction.

The graph in Fig. 5 portrays the response of the dimensionless temperature with rising values of the Biot number $\zeta$ (corresponding to convective heating). Evidently, a rise in the magnitude of $\zeta$ faciltates a rise in temperature profile as noted in this figure. Basically, a rise in $\zeta$ indicates that the internal heat transfer resistance of the sheet is more than that of the surface of the sheet. In view of this, there is a rise in the temperature as $\zeta$ advances, this response is in line with the report of Waqas *et al.* (2016) and Rahman (2011) who studied linear surface velocity (i.e $p$ =1)

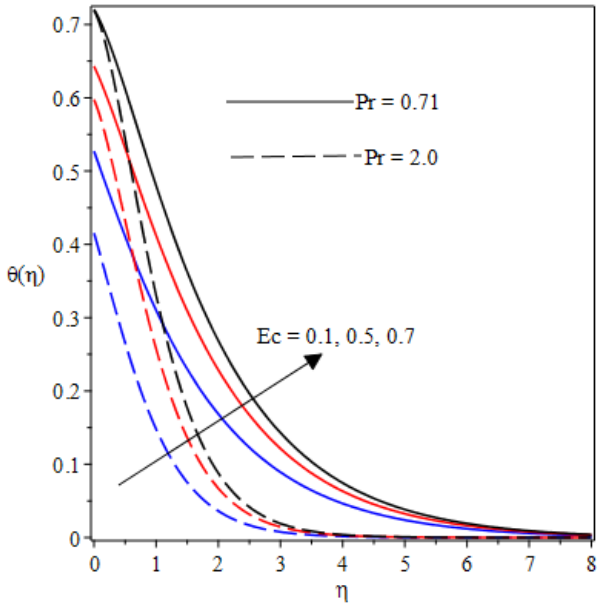


**Fig. 4** Impact of $Ec$ & $Pr$ temperature field

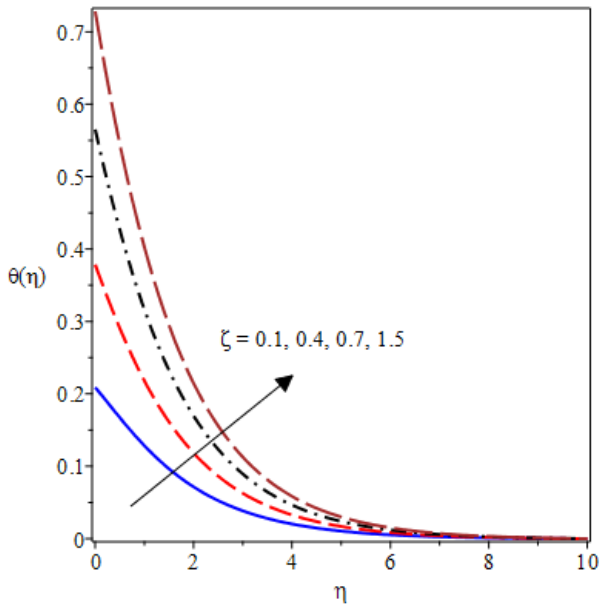


**Fig. 5** Effect of $\zeta$ on temperature profiles

Figs. 6 and 7 demonstrate the influence of the Prandtl number Pr on entropy generation and Bejan number respectively. It clearly observed that the entropy generation $Ns$ is an icreasing function of $Pr$ as depicted in Fig. 6. This response may be attributed to a rise in the temperature gradients due to rising values of Pr across the boundary layer. However, there is a decline in the Bejan number number with increasing values of $Pr$ as displayed in Fig. 7.

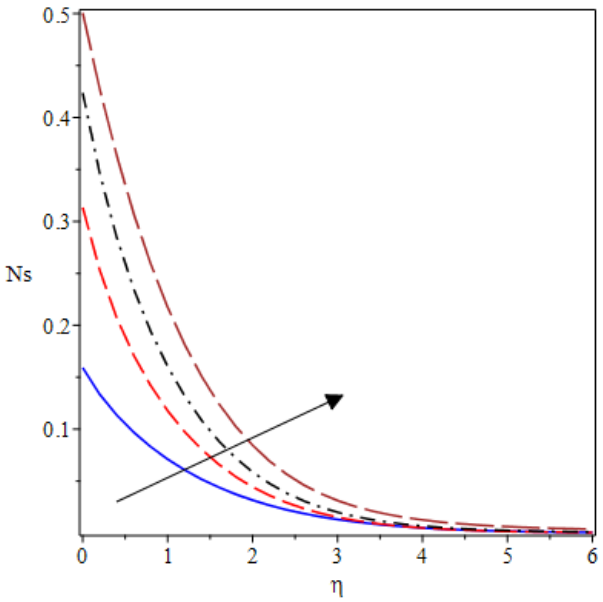


**Fig. 6** Entropy generation for variation in Pr

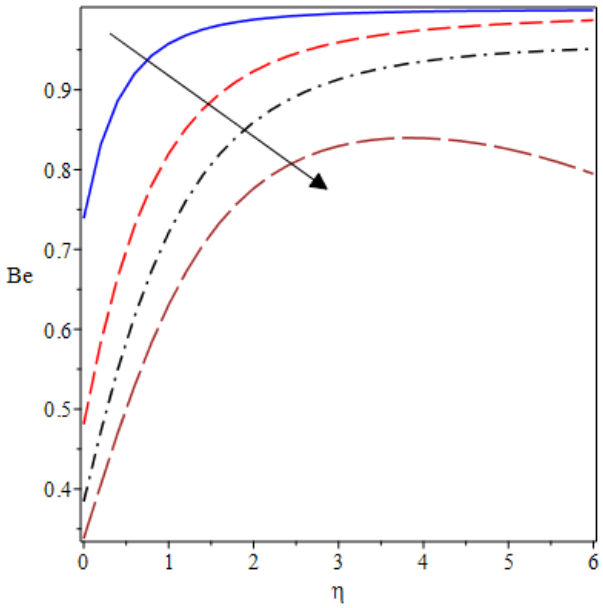


**Fig. 7** Effect of *Pr* on Bejan number

The reaction in Fig. 7 clearly shows the dominance of the irreversibility due to magnetic field intensity and the viscous dissipation owing to fluid friction over that of heat transfer irreversibility. These reactions are equivalent to the observation of of Afridi *et al*. (2017).

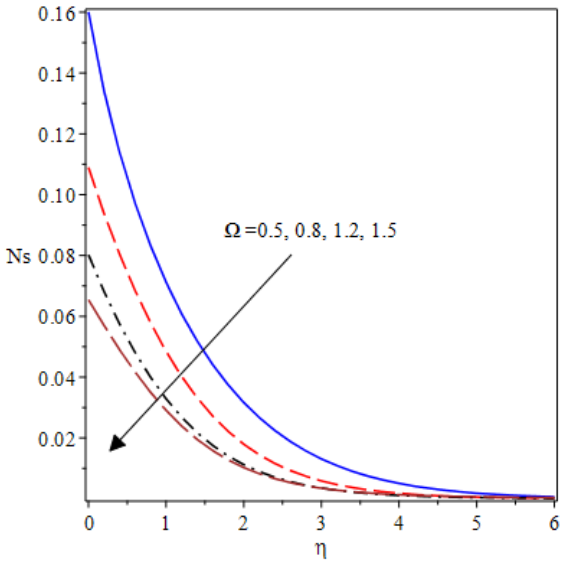


**Fig. 8** Variation of Ω on entropy generation

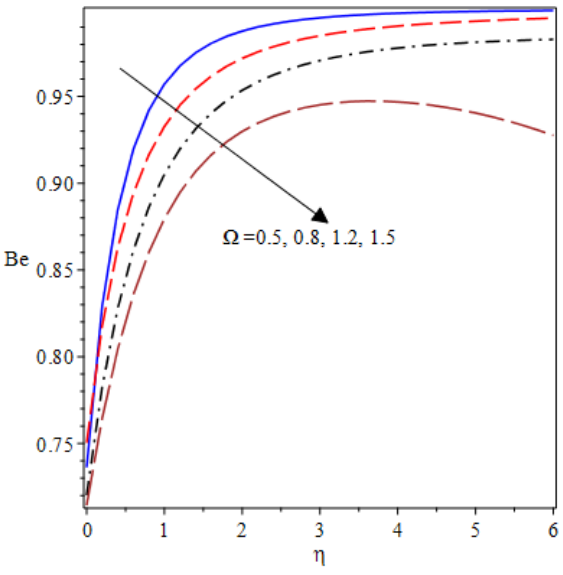


**Fig. 9** Effect of Ω on Bejan number

The graph of changes occuring in the dimensionless temperature difference Ω withh entropy production is displayed in Fig. 8 while Fig. 9 portrays that of Bejan number *Be* response to variation in Ω. In Fig. 8 a rise in Ω provides a diminishing effect on the entropy production and

hence acts against loss of available energy in the system. Meanwhile, an increase in the value of Ω ensures that heat transfer irreversiblity is lower than that of fluid friction and magnetic field intensity in the total entropy production. This is because there is a fall in the Bejan number for rising values of Ω as shown in Fig. 9.

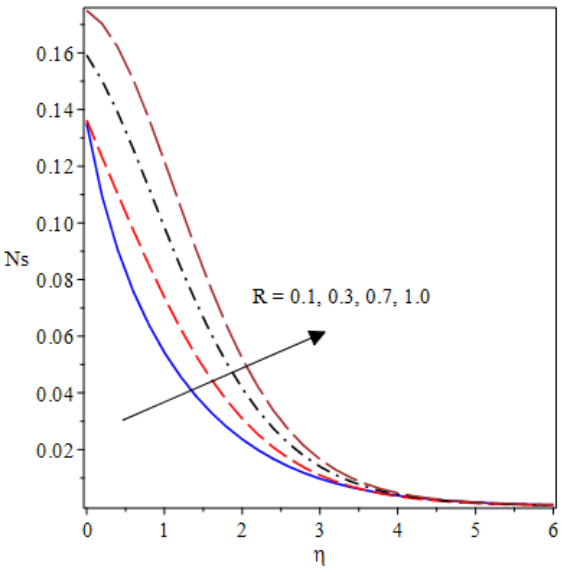


**Fig. 10** Variation of R on entropy generation

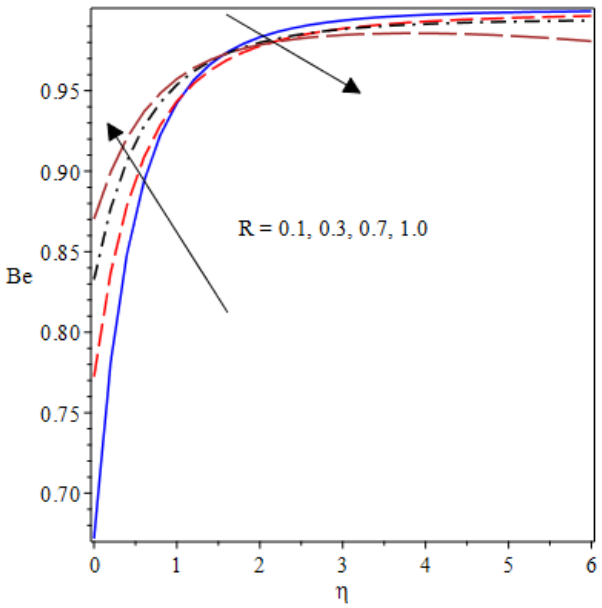


**Fig. 11** Effect of $R$ on Bejan number

The influence of radiation parameter on the entropy production is sketched in Fig. 10. It is shown that with rising values of $R$, the entropy generation rate is increasing. Hence, radiation should be reduced in order to minimize entropy production.

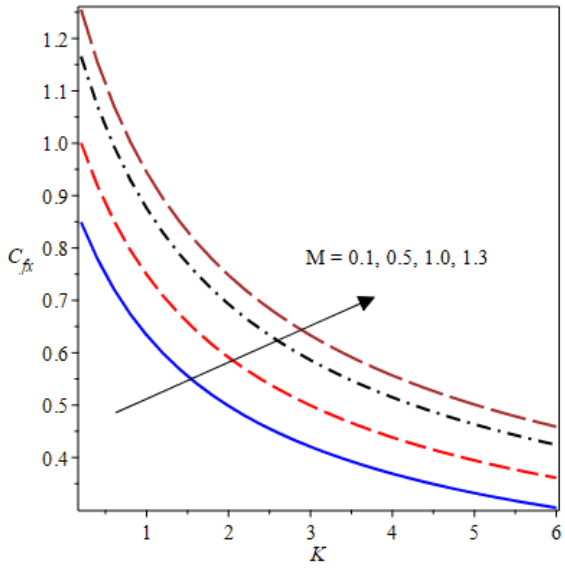


**Fig. 12** Variation of $M$ & $K$ on $C_{fx}$

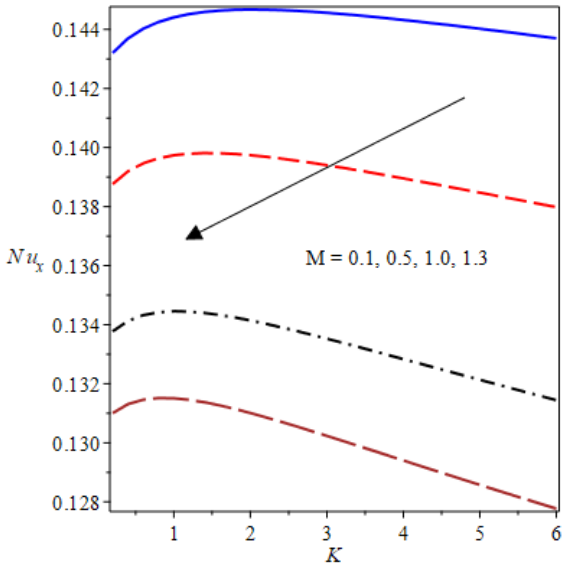


**Fig. 13** Effect of Variation of $M$ & $K$ on $Nu_x$

Meanwhile, the Bejan number rises near the stretching sheet with stronger heat transfer effect but away from the sheet, the opposite trend is noticed as noted in Fig.11.
Fig. 12 reveals that a rise in the magnetic field term $M$ tends to strenthen the skin friction coeffient $C_{fx}$ whereas for any fixed value of $M$, an increase in the material parameter $K$ lowers $C_{fx}$. Hence, application of micropolar fluid can help to reduce the viscous drag along the stretching sheet. On the contrary, Fig. 13 shows that the heat transfer at the surface of the stretching sheet decreases with a rise in $M$

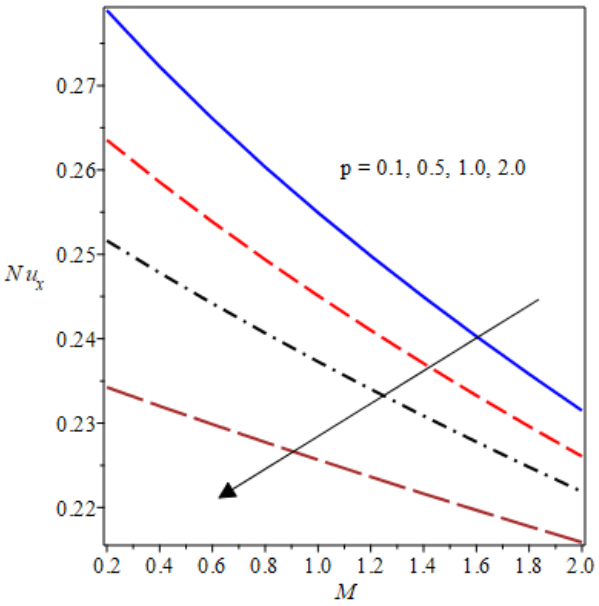


**Fig. 14.** Variation of $M$ & $p$ on $Nu_x$

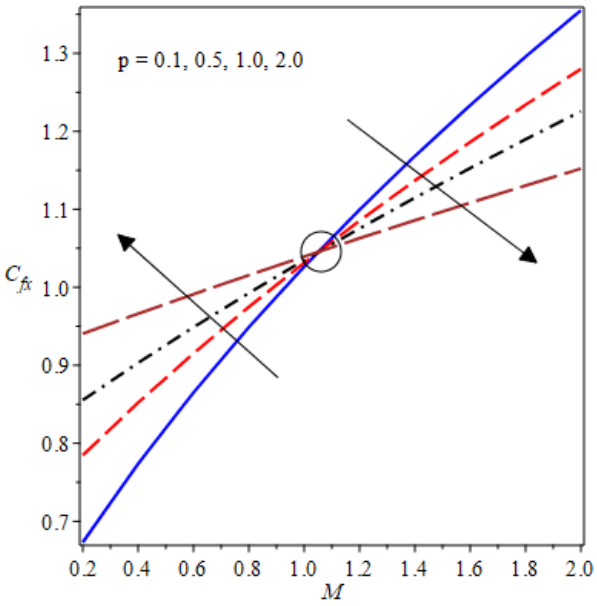


**Fig. 15.** Effect of Variation of $M$ & $p$ on $C_{fx}$

The reaction of the Nusselt number to rising values of the magnetic field parameter $M$ in the presence of the nonlinear stretching parameter $p$ is described in Fig. 14. Observation in Fig. 14 shows that heat transfer drops as the magnitude of $p$ increases. Meanwhile, the skin friction coefficient $C_{fx}$ advances with a rise in $p$ for lower values of $M$ $as$ indicated in Fig. 15, with higher values of $M \approx 1.1$ however, a rise in $p$ tends to lower $C_{fx}$.

## 5.0 Conclusion

The problem of entropy generation in hydromagnetic micropolar fluid flow along a nonlinear stretching sheet with convective heating boundary condition has been studied in the current work. The equations governing the model are formulated and converted into ordinary differential equations and then solved by means of shooting techniques alongside Runge-Kutta algorithm. The effects of the main controlling parameters have been discussed using various graphs. The results obtained also have strong relationship as validated with the published related exixting work in literature for limiting cases. From the study, it is deduced that

- The use of micropolar fluid facilitates the reduction in the viscous drag while the magnetic field influence is to boost the skin friction coefficient.
- The nonlinear stretching parameter tends to diminish transfer of heat at the sheet surface whereas the skin friction coefficient is raised with rising values of the nonlinear stretching

parameter especially with lower values of $M$

- The irreversibility owing to viscous dissipation and Joule heating is stronger than that heat transfer irreversibility with a rise in $Pr$ and non-dimensional temperature difference $\Omega$ terms while the reverse is the case for a rise in radiation term $R$ especially near the wall.
- The velocity field declines with rising values of magnetic field term $M$ in view of Lorentz force, howbeit, the temperature field advances with M while declining for growth in Prandtl number $Pr$.
- The thermal field is strengthened with growing values of Eckert number and convective heating tern $\zeta$ while it becomes weak with rising values of $Pr$.

## REFERENCES


Afridi, M. I., Qasim, M., Khan, H. and Shafie, S. (2017). Entropy generation in magnetohydrodynamic mixed convection flow over an inclined stretching sheet. *Entropy, 19*, 1-11.

Anuradha, S. and Punithavalli, R. (2019). MHD boundary layer flow of a steady micropolar fluid along a stretching sheet with binary chemical reaction. *Int J Appl Eng Res 14*, 440-446.

Arifuzzaman, S. M., Mehedi, F. U. Al-Mamun, A., Biswas, p., Islam, R. and Khan, S. k (2018). Magnetohydrodynamic micropolar fluid in presence of nano particles through porous plate: A numerical study. *Int J Heat Tech, 36*, 936-948.

Bejan, A. (1982). Second law analysis in heat transfer and thermal design, *Adv. Heat Transf., 15*, 1-58.

Bejan, A. (1996). *Entropy Generation Minimization*, CRC: Boca raton, FL, USA.

Chaudhary, R. C. and Jha, A. K. (2008). Effects of chemical reactions on MHD micropolar fluid flow past a vertical plate in slip-flow regime. *Appl. Math. Engl. Ed., 29*(9): 1179-1194.

Chen, J., Liang, C. and Lee J. D. (2011). Theory and simulation of micropolar fluid dynamics. *J. Nanoengineering and Nanosystems, 224*, 31-39.

Cortell, R. (2008). Effects of viscous dissipation and radiation on the thermal boundary layer over a nonlinearly stretching sheet. *Physics Letters A, 372*, 631-636.

Crane, L. J. (1970). Flow past a stretching plate. *Communicatios Breves, 21*, 645-647.

El-Aziz, M. and Saleem, S. (2019). Numerical Simulation of Entropy Generation for Power-Law Liquid Flow over a Permeable Exponential Stretched Surface with Variable Heat Source and Heat Flux. *Entropy, 21*, 1-19.

Eringen, A. C. (1966). Theory of micropolar fluids. *J. Math. Anal. Appl., 16*, 1-18.

Eringen, A. C. (1972). Theory of thermo-microfluids. *Journal of Mathematical Analysis and Applications, 38*, 480-496.

Fatunmbi, E. O. and Fenuga, O. J. (2017). MHD micropolar fluid flow over a permeable stretching sheet in the presence of variable viscosity and thermal conductivity with Soret and Dufour effects. *International Journal of Mathematical Analysis and Optimization: Theory and Applications, 2017,* 211- 232.

Gupta, P. S. and Gupta, A. S. (1977). Heat and mass transfer on a stretching sheet with suction or blowing. *Can. J. Chem. Eng., 55*, 744-746.

Hayat, T., Mustafa, M. and Obaidat, S. (2011). Soret and Dufour effects on the stagnation point flow of a micropolar fluid toward a stretching sheet. *Journal of Fluid Engineering, 131*, 1-9.

Hayat, T. and Abbas, Z. and Javed, T. (2008). Mixed convection flow of a micropolar fluid over a non-linearly stretching sheet. *Physic Letter A*, 372, 637-647.

Ishaq, M, Ali, G., Sha, Z., Islam, S. and Muhammad, S. (2018). Entropy generation on nanofluid thin film flow of Eyring-Powell fluid with thermla radiation and MHD on an unsteady porous

stretching sheet. Entropy, 20, 1-25.
Kobo , N. S. and Makinde, O. D. (2010). Second law analysis for variable viscosity reactive Couette flow under Arrhenius kinetics. *Mathematical Problems in Engineering, 2010*, 1-15.
Lu, D., Ramzan, M., Ahmadi, S. Chung, J. D. and Farooq, U. (2018). A numerical treatment of MHD radiative flow of micropolar nanofluid with homogeneous-heterogeneous reactions past a nonlinear stretched surface. *Scientific Reports, 8*, 1-17, Doi:10.1038/41598.018-30965
Lukaszewicz, G. (1999). *Micropolar fluids: Theory and Applications* (1st Ed.). Birkhauser, Boston.
Makinde, O. D. (2012). Entropy analysis for MHD boundary layer flow and heat transfer over a flat plate with convective boundary condition. *Int. J. Energy, 10*(2), 1-11.
Makinde, O. D., Khan, Z. H., Ahmad, R and Khan, W. A. (2018). Numerical study of unsteady hydromagnetic radiating fluid flow past a slippery sheet embedded in porous medium, *Physics of Fluids, 30*, 1-7.
Panigrahi, S., Reza, M. and Mishra, A. K. (2015). Mixed convective flow of a Powell_Eyring fluid over a nonlinera stretching surface with thermal diffusion and diffusion thermo. *Proedia Engineering, 127*, 645-651.
Rashidi, M. M. and Abass M. A. (2017). Effect of slip conditions and entropy generation analysis with an effective Prandtl number model on a nanofluid flow through a stretching sheet. *Entropy, 19*, 1-15.
Rahman, M. M. (2009). Convective flows of micropolar fluids from radiate isothermal porous surface with viscous dissipation and joule heating. *Commun Nonlinear Sci. Numer Simulat, 14*, 3018-3030.
Reddy, P. and Chamkha, A. J. (2016). Soret and Dufour effects on MHD heat and mass transfer flow of a micropolar fluid with thermophoresis particle deposition. *Journal of Naval Architecture and Marine Engineering, 2016*, 1-11.
Reena and Rana, U. S. (2009). Effect of Dust Particles on rotating micropolar fluid heated from below saturating a porous medium. *Applications and Applied Mathematics: An International Journal. 4*, 189-217.
Sakiadis, B. C. (1961). Boundary layer behaviour on continuous solid surfaces: II The boundary layer on a continuous flat surface. *A.I.Ch.E.J. 7*, 221-225.
Salawu, S. O. and Fatunmbi, E. O. (2017). Inherent irreversibility of hydromagnetic Third-grade reactive Poiseuille flow of a variable viscosity in porous media with convective cooling. *Journal of the Serbian Society for Computational Mechanics, 11*(1), 46-58.
Salawu, S. O., Kareem, R. A. and Shonola, S. A. (2019). Radiative thermal criticality and entropy generation of hydromagnetic reactive Powell-Eyring fluid in saturated porous media with variable conductivity. *Energy Reports, 5*, 480-488.
Salem. A.M. (2013). The Effects of Variable Viscosity, Viscous Dissipation and Chemical Reaction and Heat and Mass Transfer of Flow of MHD Micropolar Fluid along a Permeable Stretching Sheet in a Non-Darcian Porous Medium, *Mathematical Problems in Engineering*. 1-10.
Srinivasacharya, D. and Bindu, K. H. (2017). Entropy generation of micropolar fluid flow in an inclined porous pipe with convective boundary conditions. *Sadhana, 42*(5), 729–740.
Ullah, I., Shafie, S. and Khan, I. (2017). Effects of slip condition and Newtonian heating on MHD flow of Casson fluid over a nonlinearly stretching sheet saturated in a porous medium. *Journal of King Saud University Science*, 29, 250-259.
Vajravelu, K. (2001). Viscous flow over a nonlinearly stretching sheet. *Appl. Math. Comput., 124*,
Waqas, M., Farooq, M, Khan, M Alsaedi, A., Hayat, T., Yasmeen, T. (2016). Magnetohydrodynamic (MHD) mixed convection flow of micropolar liquid due to nonlinear stretched sheet with

convective condition. *International Journal of Heat and Mass Transfer 102*, 766–772.